Nickel-Hydrogen Cold Fusion by Intermediate Rydberg State of Hydrogen: Selection of the Isotopes for Energy Optimization and Radioactive Waste Minimization

Stoyan Sarg - Sargoytchev
World Institute for Scientific Exploration
http://instituteforscientificexploration.org

The main objection against cold fusion is based on the theoretical understanding that the Coulomb barrier of the very small nucleus is extremely strong. The size of the atomic nucleus is determined by scattering experiments in which a metal target is usually struck by alpha particles. These experiments yield only energy and angular resolution and their interpretation rely on the assumption that the atomic nuclei and all elementary particles are spherical. A non-spherical nucleus made of thinner non-spherical particles like a torus or a twisted or folded torus will provide similar data for a limited range of the particle energy. At the time of Rutherford, alpha particles with energy from 4 to 8 MeV were used. Modern scattering experiments with energy above 25 MeV show a sharp deviation from the Rutherford theory. They also show a wavelike shape of the scattering cross section as a function of scattering angle. A new interpretation of the scattering experiments leads to the idea that the Coulomb field near the nucleus has a manifold shape with a much larger overall size and therefore is not so strong. The BSM-SG models of atomic nuclei are in excellent agreement with this conclusion. Applying the approach described in the monograph Structural Physics of Nuclear Fusion with BSM-SG atomic models, the highly exothermal process between nickel and hydrogen is analyzed. It leads to the conclusion that a proton capture may occur at an accessible temperature in a range of a few hundred degrees. The process is assisted by an intermediate state of hydrogen, known as the Rydberg atom, the magnetic field of which interacts constructively with the recipient nucleus if it is in a proper nuclear spin state. The final conclusion is that it is theoretically possible to obtain nuclear energy without radioactive waste by proper isotope selection of involved elements.

Keywords: cold fusion, LENR, Coulomb barrier, nuclear energy, radioactive waste

1. Introduction

Twenty four years after the Fleischmann and Pons experiments [1] the interest in cold fusion as a promising source of nuclear energy did not dye. The skepticism against this possibility is based on the orthodox understanding of nuclear fusion. For this reason the research in this field is often referred as a Low Temperature Nuclear Reactions (LENR). The recent progress of a highly efficient exothermal reaction between nickel and hydrogen in the E-cat reactor of Andrea Rossi [2,3] and the Hyperion reactor of the Defkalion (now DGT Corp.) [4,5] put into doubt the long time belief that cold fusion is impossible. In both types of reactors a nickel nanopowder is used, while the isotope composition and reaction environments are different. To reconcile with the experimental results, main stream science has to choose between two options: (a) adoption of some abstract explanation or (b) change of some theoretical models in nuclear physics.

The followers of option (a) usually suggest theories with some foggy explanations without practical considerations for selection of the elements and the reaction environment [6]. Some theories, for example, suggest an explanation based on a Bose-Einstein condensate [7,8]. A separate example is the Windom – Larsen (W-L) theory (2005) [9], suggesting an explanation with the assumption that slow neutrons are involved. The authors speculated that the needed slow neutrons are created by interaction between a proton and a "heavy" electron. For this purpose, however, the electron must be accelerated to nearly the speed of light. In order to fit this assumption to the reaction environments of LENR experiments that use metal hydrates, W-L theory suggests the existence of a super-strong electrical field of 6.86×10^{11} (V/m) as a result of hypothetical collective oscillations of protons. At the same time, Windom and Larsen acknowledged that the detection of these slow neutrons might be

impossible. The W-L theory cannot provide explanations of three important problems for production of slow neutrons inside the nickel nanopowder: the short path for acceleration of the electron inside of the nickel nanopowder, the enormous energy required for the super fast acceleration of the electrons, and the energy for invoking the proton collective oscillation. If a correct energy balance were computed, they might come to the conclusion that energy equivalent to millions of degrees is needed – similar to the existing hot fusion model.

Option (b) (change of some existing models in nuclear physics) is painful for many theorists, but it might provide useful practical considerations. The need for such an approach was clearly expressed by Peter Gluck at Asti Workshop devoted to cold fusion (1997) [10] just nine years after the announced experiments of Fleischmann and Pons [1]. Such an approach was adopted in the Basic Structures of Matter – Supergravitation Unified theory (BSM-SG) published as a monograph in 2002 [11], then as a book in 2005 [12], while the first articles appeared in 2002 and 2003 [13,14].

2. Theoretical base of the objections against cold fusion

Why nuclear fusion is considered impossible at accessible temperatures? The quantum mechanical (QM) models of atoms are based on the Rutherford-Bohr planetary model of hydrogen. The nuclear size is determined by scattering experiments, while the nuclear shape for all **atoms** is assumed spherical and solid (without geometrical shape and structure). Using this assumption Rutherford provided a theory that led him to obtain a nuclear radius of 3.4×10^{-15} (m) from scattering experiments using alpha particles with energy in the range of 4-8 MeV [15]. A few decades later a sharp deviation from the Rutherford theory was found when using alpha particles with energy above 25 MeV (to be discussed later).

For obtaining fusion between two nuclei, their Coulomb barriers must be overcome. For a small spherical nucleus in the order of a femptometer, the estimated Coulomb barrier is so high that the two nuclei must collide with energy corresponding to a temperature in the order of millions of degrees. This process, known as hot fusion, is accepted to exist only in the stars. The first elaborate theoretical work about stellar nucleosynthesis was made by G. Gamow (1928) and A. Sommerfeld (1939). The Gamow factor is a quantum mechanical formula that gives the probability of bringing two nuclei sufficiently close for the strong nuclear force to overcome the Coulomb barrier. Therefore the Gamow factor is strongly dependent on the physical size of the nucleus, so for a nuclear size in the range of a femptometer, the estimated probability for obtaining cold fusion at an accessible temperature is zero. This theoretical understanding is valid also for the controversial nuclear process known as proton capture, which is accepted to exist in stars. Now forced by overwhelming experimental evidence for highly exothermic processes, the main theoretical opposition embraces the idea that LENR is possible only with slow neutrons. This is a known process that takes place in nuclear reactors. In many LENR experiments, however, neutrons are not detected, so this fact is used as another objection against the feasibility of cold fusion.

On one hand, the problem is the extremely small nucleus obtained by data interpretation of scattering experiments. On the other hand, not only LENR experiments but the progress in nanotechnology also indicates that the QM models of atoms are not enough useful because lacking the dimension of length. From the time of its introduction, quantum mechanics abdicated from the logical explanations based on classical electrodynamics and adopted the approach known as the Copenhagen interpretation. There was a warning about this approach even by Albert Einstein in 1922 after he developed the general relativity [16, pages: 19, 20, 23], but the opinion prevailed that human logic fails in quantum mechanics and should be replaced by mathematical logic. This opened a broad venue of abstract models but their fast development brought also some unexplained problems and logical inconsistencies. The Bohr planetary model of hydrogen was adopted at the beginning of the creation of QM and its problems were inherited by the QM models of atoms. Some of them are listed below.

- What is the size of the excited atoms before ionization (Rydberg state)? This refers to the boundary definition of an excited atom, which is problematic for QM models, especially for hydrogen.
- Why does the orbiting electron not radiate?
- Is there a classical explanation for the constant electrical charge?
- What defines the spin of elementary particles, while they are regarded as spherical?
- How can one explain the nuclear spin and spin number if the nucleus is spherical?
- Why does the Periodic table have such a shape with separated rows of Lanthanides and Actinides?
- Why are some isotopes stable and others not?
- What is the physical condition defining the length and angular direction of the chemical bonds?
- Why does the neutron have a magnetic moment and the electron - anomalous magnetic moment?

It is known that QM models explicitly deal only with energy levels. Any attempt to use physical dimensions of length leads to enigmatic problems. The imposed belief that human logic fails in quantum mechanics is an obstacle in the search for new explanations and revisions of adopted models.

3. On the need for a new interpretation of scattering experiments

The first scattering experiments provided by H. Geiger and E. Marsden in 1909 [17] are illustrated in Fig. 1. a., while their interpretation by Rutherford (1911) [15] is shown in Fig. 1.b.

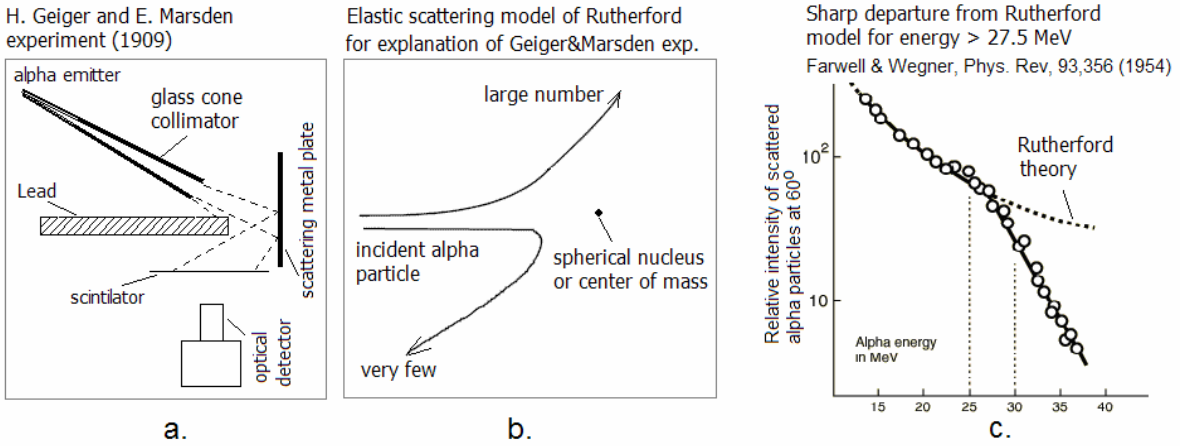

Fig. 1. a. - first scattering experiment by Geiger and Marsden, b- Rutherford interpretation, c – curve according to the Rutherford theory (dashed line) and the departure for high energy alpha particles (thick line with circles).

At the time of Rutherford, alpha particles (positively charged He nuclei) from radioactive sources were used. Their energy was in a range of 4 to 8 MeV (well below 25 MeV). In this case the alpha particle cannot come very close to the nucleus as illustrated in Fig. 1.b. The estimation of the nuclear radius by Rutherford theory relies on the extrapolation of the theoretical curve, shown in Fig. 1.c by the dashed line. The shape of the nucleus in the interpretation of scattering experiments so far is considered spherical. However, if it has another shape, such as a thinner torus, a twisted or folded torus, or a manifold combination with the same mass, the interpretation of scattering experiments below 25 MeV will provide a result similar to one obtained by Rutherford. The first evidence of departure from Rutherford theory was found by E. S. Bieler in 1924 [18] by studying the angular distribution. In 1950, Gove at al. at the MIT cyclotron provided scattering experiments with alpha particles at 27.5 MeV and observed a sharp deviation from Rutherford theory (unpublished but mentioned by R.M. Eiseberg and C. E. Porter [20]). Then extensive experiments were done by G. W. Farwell and H. E. Wegner [19]. Not only a deviation from the Rutherford theory, but also a clear wavelike dependence on the scattering angle was observed. A good summary of the scattering experiments using alpha particles with energy above 25 MeV is provided by R. M. Eisberg and C.E. Porter [20]. Some selected graphical data from their article are shown in Fig. 2.

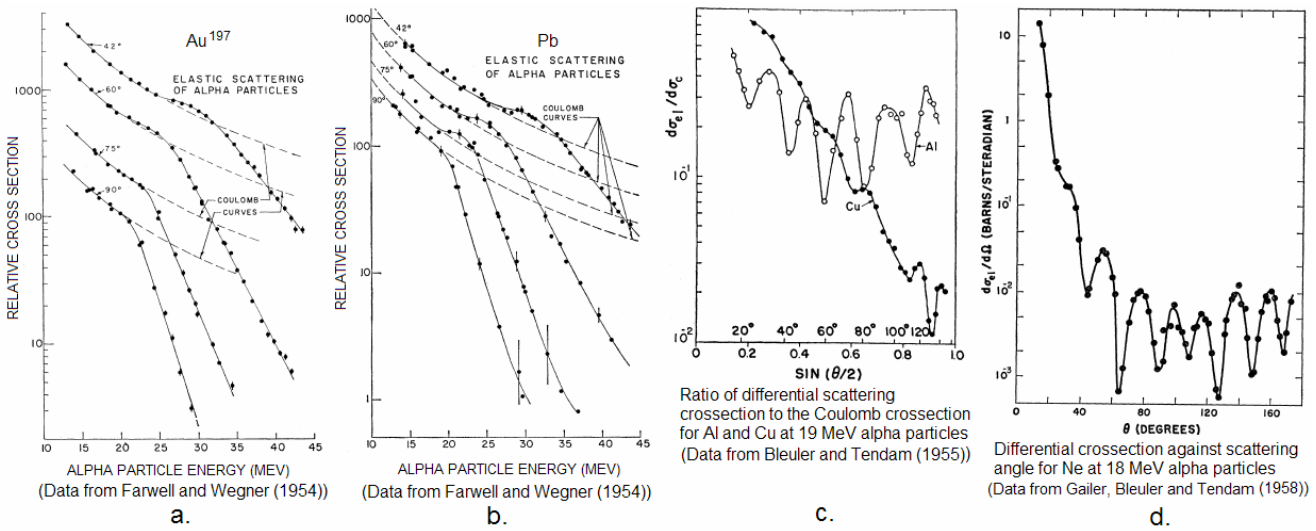

Fig.2. Graphical data from scattering experiments by alpha particles with broad energy level; a. and b – relative cross section for Al and Pb as a function of alpha particle energy; c. – ratio of differential cross section to the Coulomb cross section for Al and Cu at 19 MeV; d. - differential cross section against scattering angle for Ne at 18 MeV (From R. M. Eisberg and C.E. Porter article [20]).

Fig. 2 a. and b. show the sharp departure of the scattering data from the Rutherford theory (dashed lines) for alpha particle energy above 25 MeV. Similar data are obtained for many other elements. Later experiments show that the departure threshold slightly increases with the Z number. Fig. 2 c. and d. show another features not known at the time of Rutherford when the Rutherford-Bohr model of hydrogen was adopted as QM models of the atoms. This is a wavelike shape of the scattering cross-section as a function of scattering angle. Elastic scattering by Li nuclei provided by Badran and Al-Masri also show a similar wavelike shape dependence on the scattering angle, regarded by the authors as diffraction features [21].

In order to match the interpretation of scattering experiments to the QM model, a number of additional assumptions have been used: sharp edges of heavier nuclei and alpha particles, an opaque Akhiezer-Pomeranchuk-Clair (APB) model, a threshold range of classical and QM interpretations with the QM packet half inside and half outside of the opaque region, oscillations and damped oscillations and so on [20]. As a result, a few complex models were developed using features of an optical model with a diffraction property and many adjustable parameters. In order to obtain an acceptable fitting to the data, Badran and D. Al-Masry [21] used even more elaborate models, some of them with 20 parameters (Table 4 of the article). It is understandable that in such approach with so many adjustable parameters any kind of scattering data could be fitted to the *a priori* concept of a small structureless spherical nucleus. The opaque APB model, by the way, means an absorption by a nucleus that is a signature of the strong attractive nuclear forces for a non-spherical nucleus according to the nuclear model of the BSM-SG theory. The appearance of the sharp departure from Rutherford theory above 25 MeV means that the positively charged alpha particles exhibit some channeling effect. Fig. 3. shows scattering data by neutrons for different elements at different neutron energies [22] (data adopted from Finley at

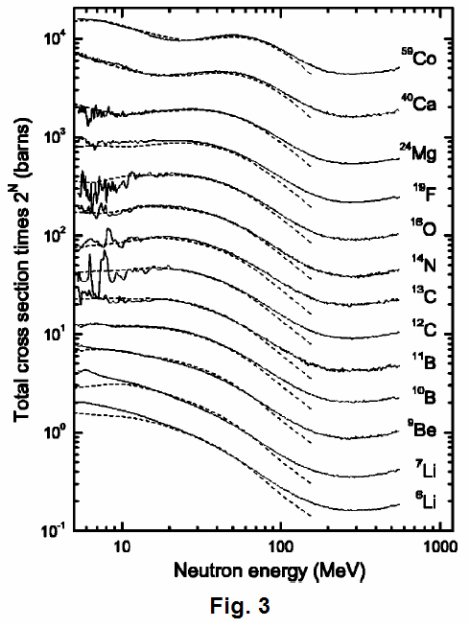

Fig. 3

al (1993)). The energy dependence of the total cross section, however, is quite different. The angular dependence of the scattering cross section by neutrons (not shown here) is also quite different.

Our analysis of old and modern scattering experiments leads to the following conclusions.

When the metal target is bombarded by alpha particles it will lose electrons and the surface will become positively charged. The existence of the wave-like shape dependency on scattering angle for alpha particles with energy above 25 MeV means that they interfere with some wave-like charge boundary. If the field of atomic nuclei near the surface having missing electrons is not spherical but has an elongated shape, the collective fields of these nuclei will interfere providing a positive wave-like field. An elongated positive near field of the nucleus is possible if the protons have an axial symmetrical arrangement. Such an arrangement will be obtained if the positive near field of the protons has an elongated shape. Some high resolution electron microscopy images show a channel structure of the metal lattice, which is in agreement with our conclusion. Such structure is apparent in Fig. 4. a and b. where high resolution electron microscope images are shown for two lattice planes of gold [23]. The transmitted pattern is from a 15 nm thick gold film. The artificial images shown in Fig 4.c were made by using the BSM-SG models, and illustrate the predicted near positive field from the atomic nuclei. In the same figure, the He nucleus is also shown for illustration of scattering by alpha particles. The wavelike near positive field of Au lattice plays a role of diffractive grating. Combined with the channeling effect it causes wavelike shape of the backscattered and trespassing alpha particles. The channeling effect permits most of the particles to pass unaffected through a thin target that provides an illusion of a very small atomic nucleus.

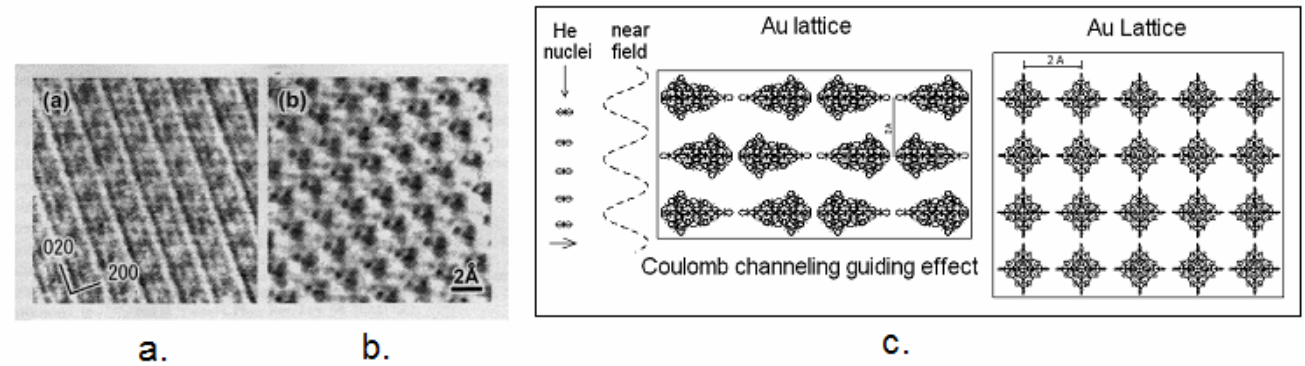

Fig. 4. a. and b. – electron microscope images of two crystal planes of Au. Courtesy of T. Kawasaki et al. [23], c. – scattering model showing the same lattice planes synthesized by BSM-SG atomic models and the near positive field induced from the collective proton charges from the proton charge

According to BSM-SG, the superdense nuclear matter causes a space microcurvature around the nucleus, which is extended to the range of Bohr radius a_0 [[24, §2.2]. This is not envisioned at the time when the Bohr planetary model of hydrogen was adopted. This feature makes the QM models consistent when working only with energy levels but not consistent if trying to work with a dimension of length. Summarizing our analysis, we emphasize the following conclusions that must be considered in data interpretation of scattering experiments:

(a) The deviation of the scattering cross section from the Rutherford theory for alpha particles with energy above 25 MeV is a result of a strong positive field gradient near the surface of the target.
(b) The wave-like shape of the scattering cross section as a function of the scattering angle is a result of interference between the positive alpha particle and a wavelike extended positive field from the nuclear charges. The effect is similar to optical interference from a diffraction grating.
(c) The data from scattering experiments show the signature of a multifold structure of atomic nuclei with a much larger size than anticipated by Rutherford theory and later models.
(d) The existence of space microcurvature is not taken into account in the data interpretation models

4. Elementary particles and atomic nuclei according to the BSM-SG theory

The Basic Structures of Matter – Supergravitation Unified Theory (BSM-SG) [11,12] is based on an alternative concept of the physical vacuum. The Supergravitational law is distinguished from Newtonian gravity in that in pure empty space the SG forces, F_{SG}, are inverse proportional to the cube of distance. It is given by Eq. (1), where C_{SG} is a SG constant, m_{01} and m_{02} are superdense SG masses

$$F_{SG} = G_{SG}\frac{m_{o1}m_{02}}{r^3} \qquad (1)$$

At very small nuclear distances, the SG forces play the role of nuclear forces, while at larger distances they propagate through the superfine structure of the physical vacuum (called the Cosmic Lattice) and become Newtonian gravitational forces. The Cosmic Lattice (CL) defines the constant speed of light, the electrical charge around the elementary particles, relativistic effects, the zero point energy and the QM properties of the particles in the CL space (physical vacuum). Detectable signatures of the SG forces are the Casimir and Van der Waals forces.

All elementary particles according to the BSM-SG theory possess superdense helical substructures, which create a charge in the physical vacuum by specific modulation of the CL structure. A proton and neutron possess one and the same such substructure, but the proton is a twisted torus, while the neutron is a double folded one. While the proton charge exists in near and far field, the charge of the neutron is locked in the near field by the SG (nuclear) forces and is not detectable, but when in motion it creates a magnetic field. The locked near field helps to study magnetic materials by neutron scattering. The shape of the proton and a neutron, and how they combine into a deuteron are shown in Fig. 5. The structure of electron is discussed elsewhere [14, 24].

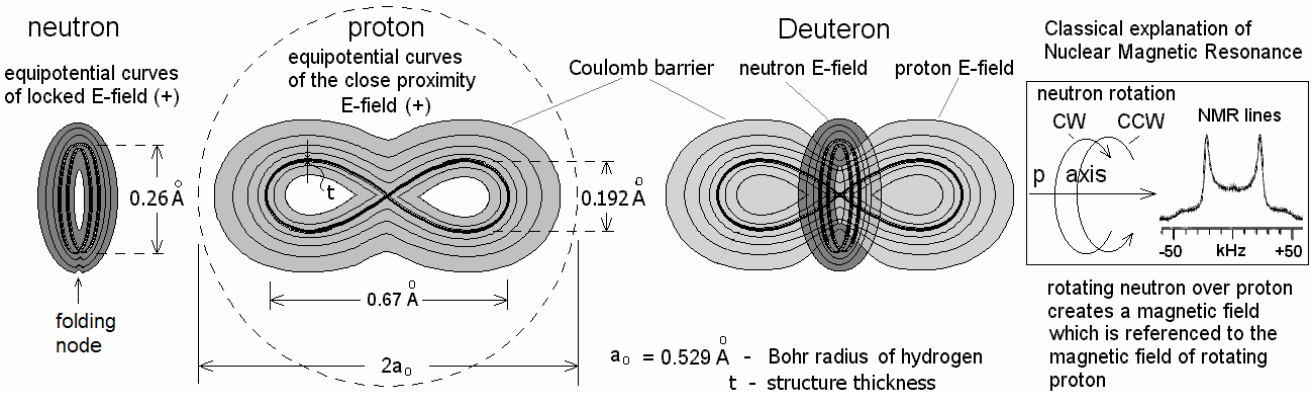

Fig. 5. Overall shape of neutron, proton and deuteron. In the decay of neutron to proton the folding node of neutron becomes a central twisting node of the proton. The right box illustrates the classical explanation of the nuclear magnetic spin of the deuterium atom (deuteron)

The double folded torus superdense structure of the neutron has a node, which should have its signature in its near field. This allows us to distinguish between the two opposite rotations referenced to its internal helical structure. They define the neutron's spin (up and down). When over the proton, the neutron is stable forming a deuteron. In the deuteron, the neutron is free to rotate over the proton, so it creates a magnetic field. This feature allows a classical explanation of the nuclear magnetic resonance and nuclear spin state as illustrated in the right-most panel in Fig. 5 (more details about nuclear spin in other elements is provided in [24, §1.3.7]). The dimensions in Fig. 5 are derived from analysis of the particle physics data, the molecular spectra, and the revealed structure and properties of the electron [11,12,14]. They are validated by the experimentally known lengths of some chemical bonds. The proton and neutron have slightly different Newtonian masses in CL space, but their SG masses are equal. By applying the SG law (1) in the model of the H_2 molecule (11,12, §9.7.4), the product of G_{SG} and the SG masses m_{01} and m_{02} (both equal, denoted as m_0) is estimated (in system SI)

$$C_{SG} = G_{SG}m_0^{\,2} = 5.26508\times10^{-33} \qquad (2)$$

Using this product, called the intrinsic SG product, the binding energy between the proton and neutron is estimated by an approximate method [11,12, §6.14.1] obtaining a value of 2.145 MeV. This theoretical value of binding energy differs from the experimental one of 2.22457 MeV by 3.6% but it gives confidence to use the intrinsic SG product, C_{SG}, for estimation of the position of the fused proton to the heavier element. The method is elaborated with application examples in [24, §1.4]

In the past few years, many scholarly articles have appeared concerning the unexplained property of cold plasma. Formation of dense clusters with peculiar properties was experimentally observed by many researchers. This formation was called **Rydberg matter** since it was associated with the Rydberg state of the atoms [33]. Since the Rydberg state is considered a highly excited level, when a high quantum number of the Bohr atom is used its size becomes unrealistically large. To avoid this, some QM models suggested a low principle quantum number, but higher angular momentum, and showed a graphical model with a highly elliptical electron orbit. But this invokes a logical inconsistency, especially for hydrogen, because the proton and electron are considered spherical and Rydberg atoms are long-lived. L. Holmlid also observed circular Rydberg electrons [34]. In contrast with QM models, the explanation of Rydberg state and Rydberg matter by BSM-SG models is extremely straight forward, as this will be briefly described below. A more detailed explanation is provided in [24,§2.4].

Fig. 6. a. shows how a proton and neutron combine in the low Z-number atomic nuclei. Fig. 6 b. illustrates the electronic orbits of the neutral hydrogen and deuterium atoms. Fig. 6.c illustrates the electronic orbit just beyond the Rydberg energy level. This is the boundary of the range inside of which the strong SG field exists. The existence of a field within this range is not envisioned by quantum mechanics because of the early adoption of the Bohr planetary model of hydrogen.

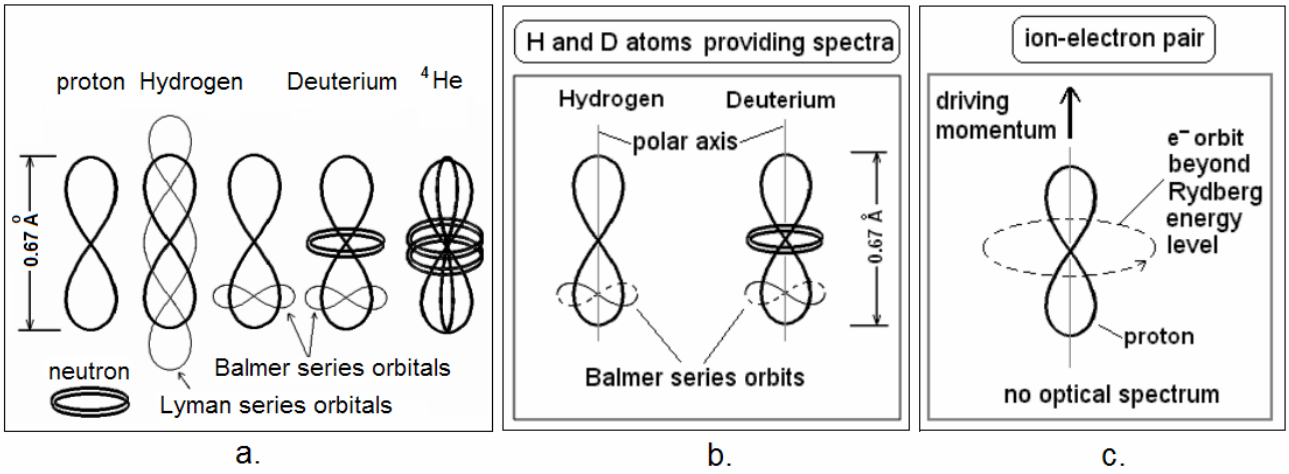

Fig. 6. a. – proton and neutron in simple atomic nuclei, b. electronic orbital in hydrogen and deuterium, c. - electronic orbit in a Rydberg atom (shown for hydrogen). The electronic orbitals are in a plane perpendicular to the drawing plane.

In a neutral atom, the electronic orbit passes through the proton's hole, as this is shown in Fig. 6. b. Since the orbit is twisted, the electron creates two opposite magnetic fields and due to the very short orbital time (shorter than the intrinsic constant of CL space) they do not appear in the far field. **This explains why the electron in a neutral atom does not radiate an EM field when circling in an orbit corresponding to one and the same energy level.** In the case of the Rydberg state, the electronic orbit is at the boundary between a neutral atom and an ion. Further, beyond this state the electron no longer passes through the proton's hole, but still rotates around it. Since it has 658 times greater magnetic moment than the proton, it creates a detectable magnetic field. The electron may move with a velocity of 13.6 eV, 3.4, eV, 1.51 eV, corresponding to quantum number 1, 2, 3 of the Bohr model of hydrogen. Using BSM-SG models, this state was called an ion-electron pair. Such

pairs are easily created in plasma and form clusters with specific magnetic properties. In the scholarly articles, this state of matter is called Rydberg matter. The activation of such clusters in plasma is invoked by the Heterodyne Resonance Mechanism discussed in the author's book [24, §2.4.5]. The described effect exists in the phenomenon glow discharge, discovered and investigated firstly by Nikola Tesla [30]. Despite the glow discharge is known for more than 100 years, some peculiar properties are not explained so far by modern physics. The magnetic property of RF activated hydrogen plasma was first reported by A. Chernetski in 1983 [31]. An ion-electron pair is a more accurate definition, but in order to match the scholarly articles, we will often refer to this state as a Rydberg state. The distance between neighboring hydrogen atoms in Rydberg matter according to some scholarly QM models is given by the empirically adjusted formula $d = 2.9n^2 a_0$, where n – principal quantum number, a_0 – Bohr radius of hydrogen. For n = 1, d = 153 pm. L. Holmlid experimentally measured the distance d for n = 1, 2, 3 and obtained values corresponding to the empirical formula [33].

Fig. 7. shows a cluster of ion-electron pairs (Rydberg matter) explained by BSM-SG models for quantum number n = 1. **The magnetic moment of the electron is 658 time the magnetic moment of the proton. Therefore, the cluster is held by the mutual magnetic interactions of the electrons which are synchronized while the individual pair moves unidirectionally (in case of strong initial momentum) or reversibly.** The distance between the ion-electron pairs is determined by the sum of the Bohr radius a_0 and the magnetic radius of the electron, derived in BSM-SG [12, §3.11] that depends on *n*. The theoretically estimated distance matches the observations made by L. Holmlid [33], and all peculiar features of Rydberg matter are directly explainable in [24, §2.4] and other BSM-SG publications elsewhere.

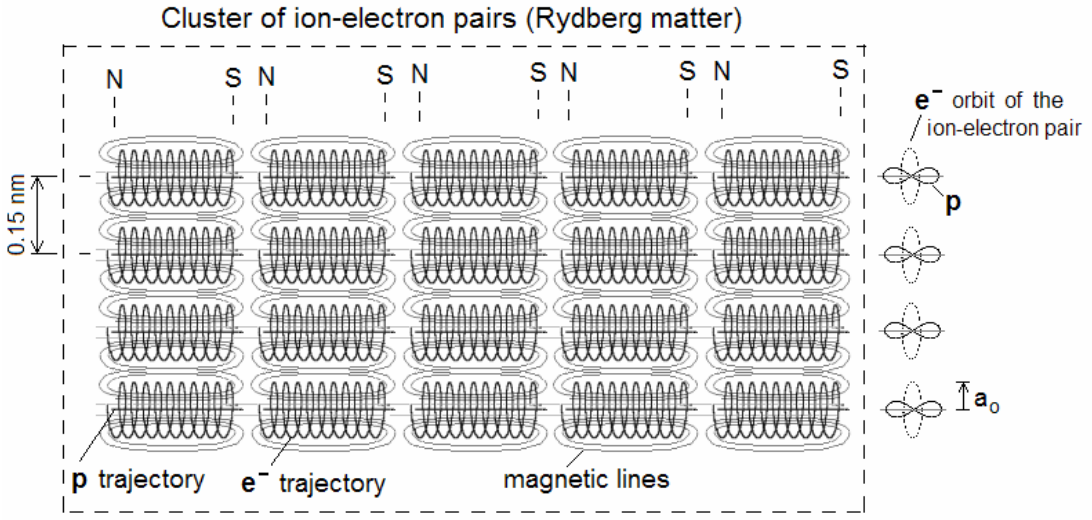

Fig. 7. Ion-electron cluster (Rydberg matter). $a_0 = 0.0529$ nm; 0.15 nm – distance obtained theoretically by BSM-SG models and measured by L. Holmlid [33].

Nuclear build-up trend of increasing Z-number

The BSM-SG models of proton, neutron and electron permit understanding of the nuclear build-up trend of the atoms, the nuclear features of the stable isotopes and why the periodic table has the Lantanides and Actinides in separate rows. The Atlas of Atomic Nuclear Structures (ANS), one of the major derivations of BSM-SG theory, provides the nuclear configuration of the stable elements in the range 1<Z<102. The spatial positions of protons and neutrons exhibit a strong trend of axial symmetry. This symmetry is important for nuclear stability. The nuclear features of the stable isotopes are discussed in [12, Chapter 8] and in [24]. The atlas of ANS is included as an appendix in the BSM-SG monographs [12,24] and published separately elsewhere.

5. On feasibility of cold fusion and selection of suitable elements and their isotopes

The issue of feasibility of cold fusion, the selection of suitable elements (and their isotopes) and the reaction environment were discussed in detail in the author's book [24] and partly in the articles [25]. The use of BSM-SG models permitted us to reveal a few important features of the atomic nuclei and physical phenomena favoring the realization of nuclear transmutations.

(a) Since the size of the proton as a twisted torus is much larger than the nuclear size adopted in QM models (due to incorrect interpretation of the scattering experiments), the Coulomb field is much weaker than one considered by QM models.

(b) The strong SG forces and the near Coulomb field of protons and neutrons are behind their packed 3D geometrical arrangement in atomic nuclei. Following this arrangement, the near Coulomb field of the nucleus obtains a multifold structure with axial symmetry.

(c) Cold fusion reaction is easier to achieve between a light nucleus like hydrogen and a recipient heavier nucleus such as Pa, Ni, Cr. The recipient nucleus must not be chemically active.

(d) The hydrogen must be activated to a Rydberg state (ion-electron pair). In this case, the proton could be preferably fused to the polar region of the recipient nucleus. The reaction is known as proton capture. It is assisted by the magnetic interaction between the Rydberg state atom and the magnetic moment of the recipient nucleus if it is in a proper spin state.

(e) The fusion process is also assisted by interaction between the Rydberg state electron (possessing a preferred energy of 13.6 eV) and the zero point energy of the physical vacuum [24, §2.5].

(f) The process of proton capture with the intermediate Rydberg state (ion-electron pair) of hydrogen occurs for the recipient atoms at the surface boundary. This requires the recipient element (Ni in the discussed case) to be in the form of a nanopowder.

The derivation of the intrinsic SG product C_{SG} given by Eq. (2) permitted development of a **method for estimation of the distance between the centers of masses** between the light and heavier recipient nuclei after the fusion, taking into account the strong SG field [24, §1.4]. This is valid also if the light nucleus is a proton (a proton capture nuclear reaction). A small correction factor is applied from the known relation of the average binding energy per nucleon as a function of number of nucleons, which is revealed to be a signature of the non-spherical shape of the nuclei [23, §1.3.6]. The method is described in §1.4 of the monograph [24] with examples §1.4.1, §1.4.3, §3.5 and Table 3.1 in [24]. The provided examples give a direct relation between the SG product C_{SG}, the distance between the center of masses (before and after the fusion) and the binding energy known from the mass deficit data.

Fig. 8. shows the method applied for the proton capture nuclear reaction between nickel and hydrogen.

$$^{62}\mathrm{Ni} + \mathrm{H} \rightarrow {}^{63}\mathrm{Cu} + \text{energy} \qquad (3)$$

The proton fused to the polar region of ^{62}Ni isotope converts it to ^{63}Cu. All input and output isotopes are stable. Consequently, this reaction leads to release of nuclear energy of 5.622 MeV without any other nuclear transmutations and radioactive waste. The nuclear reaction (3) is a proton capture. It was envisioned by Focardi and Rossi based on their extensive experimental research [1]. So far it was considered speculative because it cannot satisfy the Gamow factor criteria, estimated for a nucleus with a size in the range of femptometer scale. However such estimate is not valid for the BSM-SG models, for which the manifold Coulomb field occupies a much larger volume. Focardi and Rossi also claim that the use of isotopes ^{62}Ni and ^{64}Ni provides the most efficient output energy and they did not detect neutrons. This is in excellent agreement with our theoretical understanding of proton capture with the intermediate state of hydrogen as a Rydberg atom. The properties of this state are discussed in [24, 2.4.3] as specific features of the ion-electron pair.

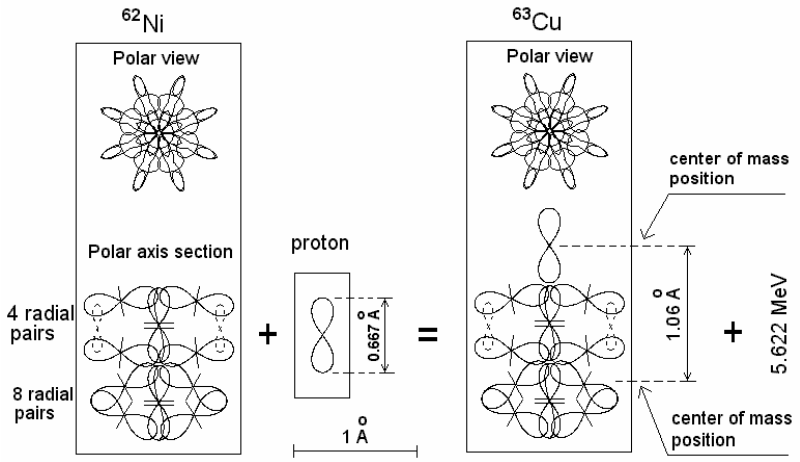

Fig. 8. Proton capture by BSM-SG models. The distance of 1.06A is calculated by the method described in [24,§1.4]. The energy estimation is from the mass deficit difference between the neutral Ni and H atoms.

Conclusion: The distance between the centers of masses after the fusion matches well with the size of the nuclei, based on the size of the BSM-SG models of proton and neutron, shown in Fig. 6.a. The knowledge of the real nuclear structure of the elements is helpful for obtaining a higher coefficient of performance by a proper selection of the isotopes of the involved elements

6. Exothermal nuclear process between nickel and hydrogen

Extensive analysis of successful experiments of cold fusion was provided in the monograph [24] and partly in article [25]. Here we will focus on the nuclear process between nickel and hydrogen that appears to be a very promising source of energy based on cold fusion. Historically the nuclear process nickel-deuterium was first investigated by Piantelli in 1990, who continued with collaborators. The history of Italian research is published in 2008 [26]. Lately the research was led by Sergio Focardi who focused mainly on nickel-hydrogen (NI-H) and in 1998 he reported an extra output power of 18 watts [27]. Then Focardi began collaboration with Andrea Rossi. Rossi developed a reactor called E-cat in which he used a nickel nanopowder with an undisclosed catalyst. This permitted raising the output heat from watts to a few kilowatts. [1]. Rossi applied for a patent in 2008 [28]. Focardi and Rossi claimed obtaining copper after a long period of operation of the E-cat reactor. In the first type of E-cat reactor demonstrated by Rossi in 2011, the hydrogen was inserted under pulsating pressure from an external hydrogen source [38]. Theoretical analysis of the two E-cat using BSM-SG models are presented in [24, §3.3] In 2012 Rossi developed a higher temperature E-cat HT. An independent test of two E-cat HT devices supplied by Rossi were made in December 2012 and March 2013 [2]. In the E-cat HT, the nickel powder is mixed with a metal hydride that releases hydrogen by heating. The nickel powder mixture with the catalyst is encapsulated in a small cylinder, which is placed in a larger cylindrical enclosure that contains heating elements and sensors. The start and stop of the nuclear process in E-cat HT was controlled by the power of the heating elements. The heat control of the second E-cat HT tested in 2013 was by a proportional temperature controller. It was found that the coefficient of performance (COP) increases with the operating temperature. It is in the range of a few hundred degrees, but must not exceed some threshold because the nickel nanopowder may deteriorate. During the tests, no radioactive radiation was detected [2]. The tests durations reported in [2] are not long enough for estimation of the burned nuclear fuel. According to one Rossi post in a blog, a 100 g of nickel was used in another 2.5 month E-cat test that delivered a continuous heating power of 10 kW [36]. In another post by Kullader and Essen who tested an earlier version of E-cat, the loaded nickel powder was 50 g. [38]. Some of the E-cat HT test results reported in [2] are shown in Table 1.

Table 1. Tests of E-cat HT1 (December 2012) and E-cat HT2 (March 2013) [2]

E-cat model of A. Rossi	Test duration [Hrs]	Average temperature ^{0}C	Input power [KW]	Output power [KW]	COP	Power density [W/kg]	Energy density [Wh/kg]
HT1	96	710	0.36	2.034	6.5	$7x10^3$	$6.8x10^5$
HT2	116	438	0.28	0.816	2.91	$5.3x10^5$	$6.1x10^7$

A successful cold fusion development based on a Ni-H mixture is provided also by the Defkalion research group founded in 2011 in Greece. In 2012 the Defkalion group was named Defkalion Green technology (DGT) and moved it's headquarter to Vancouver, Canada. The Hyperion reactor developed by DGT uses the Ni-H mixture but differs from E-cat by the reaction environment and design. The main difference is that a high voltage RF arc is used instead of catalyst. The starting and stopping of the nuclear process is controlled by the input heating and the high voltage arc. Official reports of DGT were presented at the ICCF-17 Conference in S. Korea (2012) [3] and at the ICCF-18 Conference in USA (2013) [4]. During the ICCF-18 in 2013 an 8-hr live test was run in the Defkalion laboratory in Milan, Italy and broadcasted on-line [4]. The power consumption in the nominal operational mode was 2.7 KW, while the output heat power was 5.5 KW.

According to DGT research, only even number Ni isotopes provide the heat, and only gamma radiation in the range of 50 to 300 KeV was detected [29]. According to DGT publications, a formation of Rydberg hydrogen atoms takes place, which is in agreement with our theory. One very important feature observed during the operation of the Hyperion reactor is the detectable strong magnetic field in the range of 0.6 to 1.6 Tesla. According to one published report, the magnetic peak lasts a few seconds after each high voltage pulse. An idea has been expressed that this could be from the HV plasma but this is unreasonable because the high voltage current is very small (22 mA at 24 KV) [3]. **Our conclusion is that this field is a signature of formation of ion-electron pairs arranged in clusters (Rydberg matter), as illustrated in Fig. 7. The electron trajectory has a small step defined by its anomalous magnetic moment, so the pairs are moving comparatively slowly but with a greater momentum. This is an important feature for overcoming the Coulomb barrier discussed in detail in [24, §2.4, §2.5, §2.6].**

The intermediate Rydberg state discussed for hydrogen is completely valid for atomic deuterium as well. The Japanese researchers Y. Iwamura et al. [33] reported cold fusion reactions between seven different elements and deuterium. The atomic number of the transmuted elements increased by even number of unit atomic mass. In another words, more than one deuteron was fused into the recipient nucleus according to our analysis [24, §3.8]. According to our analysis, the fusion process assisted by the intermediate Rydberg state of hydrogen (ion-electron pair) may occur not only as a single but also as a double proton capture. This explains the appearance of a small quantity of zinc as reported by Focardi [1], Rossi [28] and Defkalion [3].

7. Selection of nickel isotopes and reaction environment

From isotopic data shown in Table 2 we see that the only possible reactions in Ni-H compound that do not contribute to radioactive waste are:

$^{62}Ni + p \rightarrow {}^{63}Cu + 5.622$ MeV (4)

$^{64}Ni + p \rightarrow {}^{65}Cu + 6.946$ MeV (5)

$^{62}Ni + 2p \rightarrow {}^{64}Zn +$ gamma (5)

$^{64}Ni + 2p \rightarrow {}^{66}Zn +$ gamma (6)

Notes: (1) The estimated energy is from the mass deficit difference, not including the escape energy of electron since it is inside of the reactor; (2) The isotopes of Zn are detected in E-cat of Rossi and Hyperion of DGT.

Table 2. Isotopic data for the involved elements before and after the nuclear process

Nuclide symbol	Z(p)	N(n)	Isotopic mass	Half-life	Decay modes	Daughter isotope	Nuclear spin	Natural isotopic composition
^{H}	1	0	1.007825032	Stable			½+	0.999885
^{58}Ni	28	30	57.9353429	Stable			0+	0.680769
^{59}Ni	28	31	58.9343467	76000 yrs	EC(99%)	^{59}Co	3/2-	
^{60}Ni	28	32	59.9307864	Stable			0+	0.262231
^{61}Ni	28	33	60.9310560	Stable			3/2-	0.011399
^{62}Ni	28	34	61.9283451	Stable			0+	0.036345
^{63}Ni	28	35	62.9296694	100 yrs	Beta $^{-}$	^{63}Cu	1/2-	
^{64}Ni	28	36	63.927966	Stable			0+	0.009256
^{59}Cu	29	30	58.939498	81.5 s	Beta $^{+}$	^{59}Ni	3/2-	
^{60}Cu	29	31	59.937365	23.7 min	Beta^{+}	^{60}Ni	2+	
^{61}Cu	29	32	60.9334578	3.33 h	Beta^{+}	^{61}Ni	3/2-	
^{62}Cu	29	33	61.932584	9.673	Beta^{+}	62Ni	1+	
^{63}Cu	29	34	62.9295975	Stable			3/2-	0.6915
^{65}Cu	29	36	64.9277895	Stable			3/2-	0.3085
^{64}Zn	30	34	63.9291422	Stable			0+	0.48268
^{66}Zn	30	36	65.9260334	Stable			0+	0.27975

According to BSM-SG a hydrogen molecule H_2 could be directly converted to a pair of interconnected Rydberg state atoms. This may explain the reactions (5) and (6), but it is not sure will this lead to one or two gamma photons (to be determined experimentally). One cannot exclude the small probability for obtaining ^{63}Ni and ^{65}Ni isotopes by some conversion of a proton to neutron during the nuclear process as discussed in [24, §3.2]. Both isotopes decay by beta^{-} to the stable ^{63}Cu and ^{65}Cu. This is good for the process as discussed below, but ^{63}Ni is a long lived and may persist as a radioactive isotope in the burned nuclear fuel. Only experimental research may confirm such a possibility.

Now the question is how to invoke the Rydberg state of hydrogen. It is known that the Rydberg state could be obtained by irradiating the neutral atom by gamma or beta particles with a proper energy, or by electrical arc. The first option is evidently used in the Rossi E-cat devices, while the second one by the Defkalion group. In the case of gamma or beta radiation, the energy must not be very strong so that the electrons could not escape the positive ion. Only emitters of negative beta particles must be used because some positive beta particles will form positroniums with the electrons. These missing electrons will lead to formation of unwanted local positive charge. A suitable emitter of negative beta particles is the ^{63}Ni isotope (see Table 2). Its long half-life of 100 years means that the beta particle rate will be constant during the lifetime of the nuclear fuel. The maximum energy of the negative beta particles from ^{63}Ni is only 6.59 KeV, so they could be more easily thermalized to lower energy particles when passing through the fuel nanopowder. Instead of mixing with the fuel, the negative beta emitter could be doped to the internal surface of a cylinder with a small diameter or could be put between two cylinders with small thickness of the internal one. In this way it will not be displaced as a radioactive waste. This fits with the design chosen by Rossi for his megawatt power system made by parallel E-cat HT reactors in the KW range. ^{63}Ni is a commercially available isotope used in some electronic devices (surge protectors, modern sensors) and for some diagnostic purposes. ^{63}Ni is not considered unsafe, but it needs to be handled with caution. [35]. The maximum range of the emitted beta radiation in air is 2.14 inches so it can be easily shielded.

Functionally, the low and high temperature E-cat reactors of Rossi are distinguished from the Hyperion reactor of Defkalion. In the E-cat a beta emitter is probably used, while in the Hyperion – a HV arc. Rossi probably used an RF generator for triggering the nuclear process.

The advantages of the Rossi method are: the possibility of using a metal hydride instead of a hydrogen vessel, a more compact design, and assuring zero radioactive waste in an optimized reaction environment. The disadvantage, especially for E-cat HT, is that if running at higher temperatures for higher COP, the stopping of the process by the heat control might be difficult and may need an active cooling. This requires individual power control for each E-cat HT reactor in a parallel system.

The advantages of the Defkalion method are: an easier control, including start and stop, by control of the temperature and the high voltage arc, and a possibility to scale up for a larger power unit. The main disadvantage is the more difficult control of unwanted nuclear transmutations that may contribute to radioactive waste. The Hyperion reactor operates with pressurized hydrogen, so it is much more complicated than the E-cat HT reactor and requires more safety precautions.

Solid state metal hydrides provide a safe and efficient way of hydrogen storage. They are commercialized for use in rechargeable batteries and fuel cells. The hydrogen storage is reversible and it can be released by heat. Some of them can work at a temperature around a few hundred degrees and a pressure of tens of bars [37].

Following our analysis, a general functional block diagram for the reactor system and the nuclear process Ni-H is shown in Fig. 9.

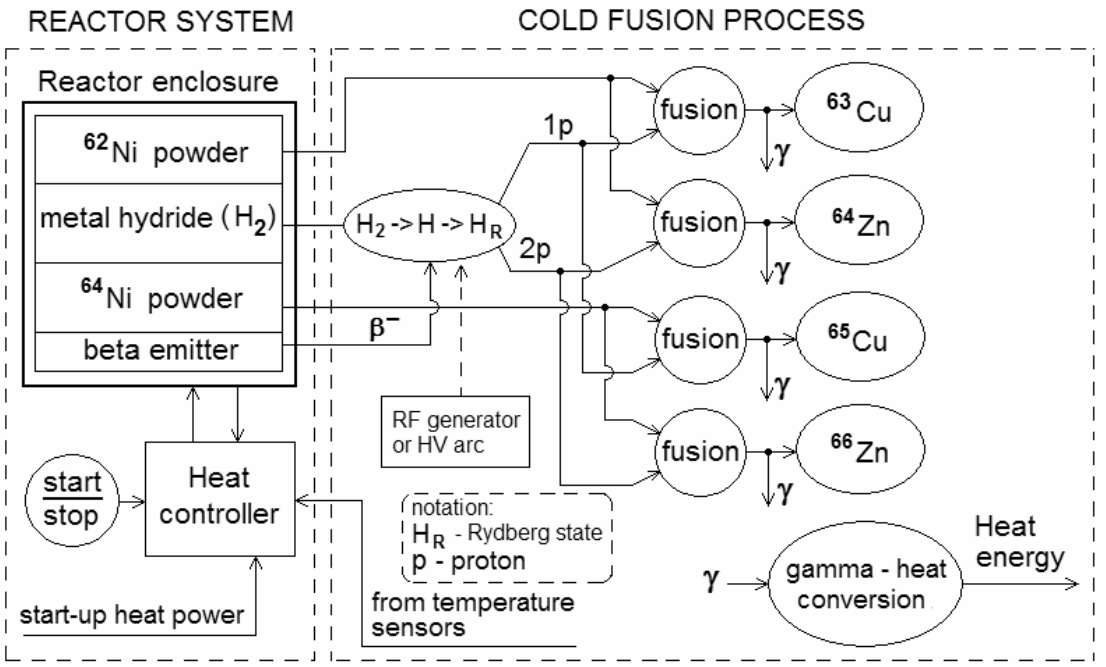

Fig. 9. Functional block diagram of reactor system for Ni-H process. In E-cat HT of Rossi a metal hydride for hydrogen storage and beta (or gamma) emitter is used. The metal hydride could be also outside of the reactor. Hyperion reactor of Defkalion uses pressurized hydrogen and a HV arc, working in on/off mode.

In the case that the metal hydride is mixed with the fuel powder, it must not be involved in nuclear reactions that produce unstable isotopes. Among the choices could be a metal hydride based on Palladium for which extensive research data are available [37]. Proton capture with Pd has a low probability but we must consider such a possibility. If the most abundant stable isotope ^{108}Pd is selected, one proton capture will lead to a stable silver isotope ^{109}Ag. Two proton capture will lead to unstable ^{110}Ag, with a half life of only 24.6 s that will decay by a β^- to the stable ^{110}Cd. The released β^- will contribute to the formation of ion-electron pairs (Rydberg state).

8. Design considerations for a cold fusion nuclear reactor

Let us discuss the design of the E-cat HT reactor of Andrea Rossi, from the point of view of our considerations. Fig. 10 shows the design of this reactor according to the descriptions provided by the patent application of Rossi [28], his on-line publications, and the test article [2]. The nuclear fuel is hermetically enclosed in a copper cylinder 3. The fuel mixture 1 contains a nuclear fuel and a metal hydride. The nuclear fuel according to Rossi is ^{62}Ni, but according to our considerations it may contain also ^{64}Ni . This is mentioned also in a Focardi and Rossi paper [1]. The metal hydride could be palladium ^{108}Pd. The catalysts according to our considerations could be ^{63}Ni, but it could also be another source of negative beta particles or a gamma emitter. It could be added to the fuel mixture or implanted on the internal surface of the copper cylinder. It could also be put between a thin cylinder (placed inside of the copper cylinder) and the copper cylinder 3. The boron ^{10}B enclosure, 4, serves to trap some neutrons that may be emitted by some unstable isotope, apparently obtained by nuclear transmutation. The lead jacket, 5, must protect from some strong gamma radiation. The copper, boron, and lead are rigidly enclosed in a steel cylinder 6 placed in a larger cylindrical enclosure of steal and silicon nitride ceramics. The latter is high temperature material capable of surviving thermal shocks. It is used in the automotive industry. Between the two cylindrical blocks are electrical heaters that are preferably controlled by a PID controller. The external surface of the E-cat HT is painted with a high temperature resistant black paint for higher emissivity.

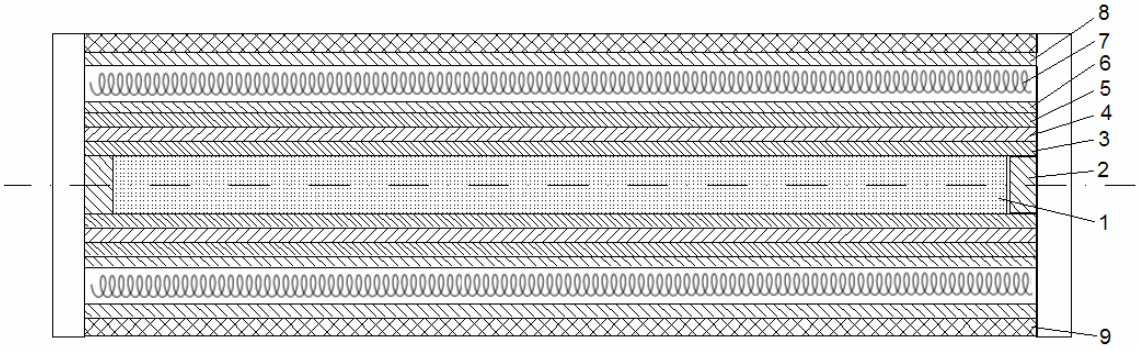

Fig. 10. E-cat HT of Andrea Rossi. 1 – a mixture of Ni powder and metal hydride, 2 caps, 3 – copper cylinder, 4 - ^{10}B isotope, 5 - lead jacket, 6 - steel cylinder, 7 – electrical heaters, 8, steel enclosure, 9 – silicon nitride ceramics

The nickel powder and the metal hydride may not withstand a temperature higher than 600 – 700 C. To avoid local overheating, the enclosure volume of the fuel mixture may need some atmosphere. It is not clear whether this could be only the hydrogen or some quantity of noble gas, for example argon. A suitable heat control is the PID (proportional integration differentiation) type. The heat controller of the E-cat HT 2 was probably of such a type.

The nickel nanopowder might need some preparation process. According to a comment by Sterling D. Allan, Pure Energy Systems News, January 17, 2011, somebody suggested that the nickel nanopowder used in E-cat must undergo the following preparation:

1) Baking and cleaning to remove oxidation from the nickel nanoparticles.
2) Bathing in acid or another compound to make the particles more porous
3) Must be eventually embedded in a membrane or ceramic structure.

The use of the Ni-H process for generation of electrical power may need a higher COP than demonstrated by the E-cat HT (see Table 1) and the Hyperion reactor of DGT. The E-cat HT tests showed that the COP increases with the operating temperature. With the temperature increase, however, the electrical heaters will consume less and less power and the process may go out of control. This in fact happened with the very first E-cat HT test and the device was destroyed [2]. For this reason, the second E-cat HT was run by a PID controller at a lower temperature. To avoid this and to stop the process, while pursuing a higher COP, an active cooling process must be used. This

could be done by using a flowing liquid. Then the maximum operating temperature will be limited by the boiling point of this liquid. One solution for a commercial product with a high COP is to use a gallium metal. Gallium is in a liquid phase above 29.76 C and its boiling point is 2204 C.

Caution: If the nickel isotopes are different from those suggested, or the metal hydride is different or different beta and gamma emitter is used or a HV electrical ark is used, the nuclear process may produce unstable isotopes. They must be properly handled and disposed.

Another predicted cold fusion process is based on chromium-hydrogen is discussed in [24, §3.7] The considerations for minimization of the nuclear waste must be elaborated in a similar way.

9. Discussion and conclusions:

This article is a continuation if the theoretical developments presented in the monograph [24] and the articles [25] permitting some useful practical recommendations in the field of cold fusion. The revision of data interpretation models of scattering experiments leads to the conclusion that the atomic nuclei possess a multifold Coulomb field with a much larger size than anticipated so far. In Ni-H and other similar LENR systems, the overcoming of the Coulomb barrier is possible if the hydrogen is in an intermediate Rydberg state (ion-electron pair according to BSM-SG theory). The process known as a proton captures is assisted by the magnetic interaction between the Rydberg matter and the nickel nuclei which are in a proper nuclear spin state. The optimization of the released nuclear energy and the minimization of the radioactive waste are possible by a proper isotope selection of the involved elements.

Disclaimer:

1. The author claims that only publicly available data published by the researchers of cold fusion (LENR) about Ni-H process were used. He did not obtain any data related to some trade secrets or proprietary information. The apparent match to some trade secrets is a result of scientific analysis of the public data by using the BSM-SG models.
2. This article is provided for the purpose of advancing scientific knowledge. The author cannot be held responsible for any injury, damage or loss of property that may eventually occur by improper experimental setup or test provided in an unsuitable environment.

Aknowledgement: As a member of the Board of Distinguished Scientific Advisors to the World Institute for Scientific Exploration, the author would like to tank to the Board of Directors for the encouragement and the moral support for this theoretical development.

References:

1. M. Fleischmann and S. J. Pons, Electroanal. Chem., v. 261, 301, (1989)
2. S. Focardi and A. Rossi, http://www.journal-of-nuclear-physics.com/?p=360
3. G. Levi et al, Indication of anomalous heat energy production in a reactor device containing hydrogen loaded nickel powder, http://arxiv.org/abs/1305.3913
4. J. Hadjichristos, M. Koulouris, A. Chatzichristos, Technical Characteristics & performance of the Defkalion's Hyperion Pre-industrial Project, ICCF-17, (2012) http://newenergytimes.com/v2/conferences/2012/ICCF17/ICCF-17-Hadjichristos-Technical-Characteristics-Paper.pdf
5. Defkalion cold fusion demo during ICCF-18, (2013) http://www.youtube.com/watch?v=HHEtnTO3h6s&feature=c4-overview&list=UUUX6cT8DJdhop_b4yp_4r_w
6. Cold fusion theories http://en.wikiversity.org/wiki/Cold_fusion/Theory
7. F. Dalfovo and S. Giorgini, Theory of Bose-Einstein condensation in trapped gases, Reviews of Modern Physics, Vol. 71, No. 3, 463-512, (1999)
8. Y. E. Kim, Generalized Theory of Bose-Einstein Condensation Nuclear Fusion for Hydrogen-Metal System, Purdue University, West Lafayette, Indiana 47907, USA Preprint PNMBTG-6-2011 (June 2011)
9. A. Widom, L. Larsen, Ultra Low Momentum Neutron Catalyzed Nuclear Reactions on Metallic Hydride Surfaces, Eur. Phys. J. C, 46, 107-111, (2006)

10. Asti Workshop on Anomalies in Hydrogen/Deuterium Loaded metals, New Energy Times, ICCF and LENR Proceedings, International Conference on Cold Fusion http://newenergytimes.com/v2/conferences/LENRConferenceProceedings.shtml
11. S. Sarg ©2001, *Basic Structures of Matter*, monograph, http://www.helical-structures.org also in: http://www.nlc-bnc.ca/amicus/index-e.html (First edition, ISBN 0973051507, 2002; Second edition, ISBN 0973051558, 2005), (AMICUS No. 27105955), LC Class no.: QC794.6*; Dewey: 530.14/2 21
12. S. Sarg, Basic *Structures of Matter – Supergravitation Unified Theor*y, ISBN 9781412083874, (2005), Amazon.com
13. S. Sarg, New approach for building of unified theory, http://lanl.arxiv.org/abs/physics/0205052 (May 2002)
14. S. Sarg, A Physical Model of the Electron according to the Basic Structures of Matter Hypothesis, Physics Essays, volume. 16, No. 2, 180-195, (2003) available in: http://vixra.org/abs/1104.0051
15. E. Rutherford, The scattering of α and β particles by Matter and the Structure of Atom, Phil. Mag. Series 6, vol. 21, p. 669-688, (1911)
16. A. Einstein, Sideligths on Relativity (1922, p.19,20,23), https://archive.org/details/sidelightsonrela00einsuoft
17. H. Geiger and E. Marsden, On a Diffuse Reflection of the α -Particles, Proc R. Soc. London, A, 82, 495-500, (1909)
18. E. S. Bieler, Large-Angle Scattering of α -Particles by Light Nuclei, Proceedings of the Royal Society of London, Series A, vol. 105, No 732, 434-450, (1924)
19. G. W. Farwell and H. E. Wegner, Elastic Scattering of Intermediate-Energy Alpha Particles by Heavy Nuclei, Physical Review, v. 95, No. 5, 1212-1217, (1954).
20. R. M. Eisberg and C.E. Porter, Scattering of Alpha Particles, Review of Modern Physics, V. 13, No 2, 190-230, (1961).
21. R. I. R. I. Badran and Dana Al-Masri, Exploring diffractive features of elastic scattering of ^{6}Li by different target nuclei at different energies, Ca. J. Phys., v. 91, 355-364, (2013)
22. W. P. Abfalterer et al., Measurement of neutron total cross section up to 560 MeV, Phys. Rev C, v. 63, 044608, (2001)
23. T. Kawasaki et al., Applied Physics letters, v.6, 459, (1977)
24. S. Sarg, *Structural Physics of Nuclear Fusion with BSM-SG atomic models* ISBN 9781482620030, (2013), Amazon.com
25. S. Sarg, Theoretical feasibility of Cold Fusion According to the BSM- Supergravitation Unified Theory, General Science Journal, http://gsjournal.net/Science-Journals/Essays/View/4805 (2013) also in Journal of Nuclear Physics (extended version) http://www.journal-of-nuclear-physics.com/?p=833 (submitted 2011 issued 2013)
26. Cold Fusion. The history of research in Italy. Italian National Agency for New Technologies, Energy and Environment, Report in, 2008. Editors S. Martelluci, A. Rosati, F. Scaramuzzi, V. Violante http://old.enea.it/com/ingl/New_ingl/publications/pdf/Cold_Fusion_Italy.pdf
27. S. Focardi et al., Large excess heat production in Ni-h system, IL Nuovo Cimento, v. 111 A, N.11, 1233-1242, (1998)
28. A. Rossi, Method and Apparatus for Carrying out Nickel and Hydrogen Exothermal Reactions, WO 2009/125444 A1 (15 Oct 2009) (patent submitted 4 Aug 2008).
29.J. Hadjichristos and P. Gluck, Heat Eenergy from Hydrogen-Metal Nuclear Interactions, Process in Isotopes and Molecules International Conference, Cluj-Napoca, Romania, 25-27 Sep (2013).
30. N. Tesla, Experiments with alternative current of high potential and high frequency, reports at Institute of Electrical Engineers, London , (1982) (Available in http://books.google.ca/books?isbn=1602060584)
31. A. B. Chernetski. Plasma systems with separated electrical charges, Moscou Institute G. V. Plehanov, (1983) (in Russian). See also in http://www.rexresearch.com/chernetskii/chernetskii.htm
32. Y. Iwamura et al., "Elemental Analysis of Pd Complexes: Effects of D_2 Gas Permeation," Jpn. J. Appl. Phys. Vol. 41 (2002) pp. 4642–4650 http://newenergytimes.com/v2/views/Group1/Iwamura.shtml
33. L. Holmid, Sub-nanometer distances and cluster shapes in dense hydrogen and in higher level of hydrogen Rydberg Matter by phase-delay spectroscopy, J. Nanopart. Res. 13, 5535-5546, (2011).
34. L. Holmlid, Direct observation OF CIRCULAR Rydberg electrons in a Rydberg matter surface layer by electronic circular dichroism, J. Phys.: Condensed Matter, v. 19. No. 27, 276206, (2007).
35. Ni-63 safety data sheet http://www.stanford.edu/dept/EHS/prod/researchlab/radlaser/RSDS_sheets/Ni-63.pdf
36. M. Felderhoff and B. Bogdanović, High Temperature Metal Hydrides as Heat Storage Materials for Solar and Related Applications http://www.ncbi.nlm.nih.gov/pmc/articles/PMC2662468/
37. W. H. Fleming Jr, Analysis of Heat Transfer in Metal Hydride Based Hydrogen Separation WSRC-TR-99-O0348, Rev. 2, (1999)
38. www.nyteknik.se/nyheter/energi_miljo/energi/article3144827.ece
39. Rothwell, J., ed. Brief Technical Description of the Leonardo Corporation, University of Bologna, and INFN. Scientific Demonstration of the Andrea Rossi ECat (Energy Catalyzer) Boiler. 2011, LENR-CANR.org. http://lenr-canr.org/acrobat/RothwellJbrieftechn.pdf